

Modelling And Simulation Of Photovoltaic Array Fed Induction Motor Based On Field Oriented Control And Single Stage MPPT Inverter For Water Pumping System

Mohamed Elsayed Elnagi Mahmoud

Electrical Engineering Department,
Al-Azhar University, Qena, Egypt,
mohamed.elnagi@azhar.edu.eg

Ahmed A. Zaki Diab

Electrical Engineering Department,
Minia University, Egypt
engahmedz@yahoo.com

Mohammad Kamal Ahmed

Electrical Engineering Department,
Al-Azhar University, Cairo, Egypt,
mkalshaar@yahoo.com

Barakat M. Hasaneen

Electrical Engineering Department,
Al-Azhar University, Qena, Egypt,
Bmhsaneen@yahoo.com

Abstract— This paper presents a photovoltaic (PV) system for water pumping. The water pumping system consists of PV array, a voltage source inverter (VSI) and 3 phase induction motor that drives the centrifugal pump. For the purpose of improving the efficiency of overall system, the incremental conductance method algorithm based Maximum Power Point Tracker (MPPT) and field oriented control scheme is applied to control the single stage of VSI fed the three phase induction motor. An incremental conductance method is used for extraction of maximum power and the vector control is used to drive motor which provides smooth startup and reducing of starting current. The proposed system could be employed in agricultural irrigation under any operating condition of varying natures of solar irradiances and temperatures. Simulation results using MATLAB/SIMULINK show that the performance of the PV/pumping system in transient as well as in steady state is quite satisfactory.

Keywords; *Photovoltaic array, MPPT, field oriented control, Centrifugal water pump.*

I. INTRODUCTION

Water pumping is an energy intensive process and most of the water pumping systems are powered by conventional energy production based on fossil fuels, which their costs are increasing, operation becomes increasingly expensive and with the additional harming the environment of pollution and greenhouse gas emissions [1-6]. So the solar energy is the best choice to provide electricity for water pumping systems in the countries and remote area because the sun will always shine on the Earth and Solar energy is a clean resource with zero emission [1]. Egypt one of the solar belt countries and it has the highest number of sunshine hours all year round with higher irradiation

levels [2]. As water is the source of life, the use of solar energy to feed water pumping systems will help to develop remote areas, which are frequently located too far away from existing electric grid lines. This helps the Desert Development and support of the Egyptian economy and turn the desert into a green oasis. As the solar cell efficiency is low, so maximum power point tracking (MPPT) technique is employed to overcome the characteristic problems of the PVs and to make PV array work efficiently and effectively in different climatic conditions. DC motors and Induction motors driven PV pumps are already in use in several parts of the world. But DC motors suffer from maintenance problems due to the presence of the Commutator and brushes. Therefore a pumping system based on an induction motor can be an attractive proposal where reliability, speed capability, robustness and maintenance-free operations with less cost are important due to absence of Commutator, slip rings and brushes. In addition, when used with a field-oriented control scheme, the induction motor can compete with the DC motor in high-performance applications [3]. In this work the modeling of PV pumping system presents based on PV array, dc link capacitor, a voltage source converter, three phase induction motor, employs maximum power point tracker (MPPT), Vector control is used for the induction machine control and water tank storage instead of batteries. PV array is built up using series and parallel connections of PV panels for matching the required power, voltage and current rating of the motor. Here a voltage source inverter (VSI) directly converts DC power to AC power, without need to DC-DC converter and delete its cost. It also makes the whole system size is reduced since there is no inductor. Also in PV pump storage system, solar energy is stored, when sunlight is available as potential energy in water tank storage and consumed according to demand instead of batteries which are heavy and expensive and have one fifth of

the lifetime of a PV panel so there are advantages in avoiding the use of large banks batteries[4]. Vector control is used for the induction machine control which improves its performance over the scalar variable frequency drive [5-8]. operating point at the intersection of current-voltage curves of the PV array and the motor-pump position may be far from the maximum power point (MPP) of the generator, so it wastes a significant proportion of the available solar power[9,10]. Therefore maximum power point tracking unit is used to optimize operation point for power extraction through controlling by decreasing and increasing of the reference speed value of Vector control during current source and voltage source region to match the PV generator to the optimum motor-pump position. Subsystems and control methods will be modeled and simulated using Matlab and Simulink with actual irradiance data. In this paper modelling, simulation and analysis of PV water pumping system has been presented. Moreover, the simulation results prove the effectivity of the proposed system.

II. MODELING OF STANDALONE PV WATER PUMPING SYSTEM.

The power configuration of the studied photovoltaic pumping system is depicted in fig. 1. Where PV array followed by inverter and three phase IMD directly coupled with the Centrifugal Pump and give required output.

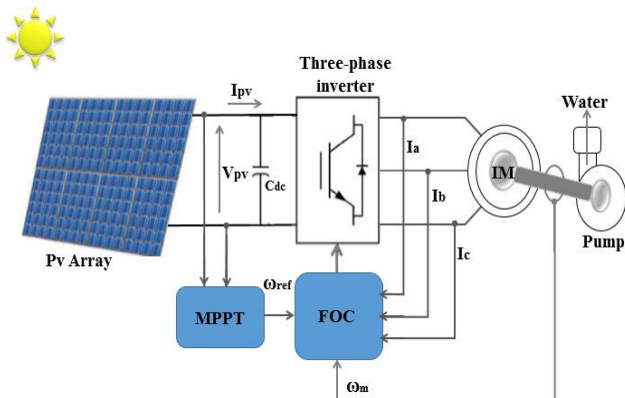


Fig. 1. Block diagram of PV pumping system

A. Photovoltaic Cell

Basically, PV cell is a P-N semiconductor junction absorb and convert sunlight into electricity. The PV cell is modeled by using the two-diode model equivalent circuit as shown in fig.2 where The circuit of PV cell consists of the photo-current source (I_{pv}) connected in parallel with a two diode [11, 12]. The following equation describes the output current of the cell [11, 13-15]:

$$I = I_{pv} - I_{o1} \left[\exp \left(\frac{V - IR_s}{a_1 V_{T1}} \right) - 1 \right] - I_{o2} \left[\exp \left(\frac{V - IR_s}{a_2 V_{T2}} \right) - 1 \right] - \left(\frac{V - IR_s}{R_p} \right) \quad (1)$$

$$V_{T1} = V_{T2} = V_T = \left(\frac{N_s K T}{q} \right) \quad (2)$$

And

$$I_{o1} = I_{o2} = I_o = \frac{(I_{sc,STC} + K_I \Delta T)}{\exp \left[\frac{(V_{oc,STC} + K_V \Delta T) / \{(a_1 + a_2) / P\} V_T}{-1} \right]} \quad (3)$$

Where $a_2 \geq 1.2$ and $a_1 = 1$ [11, 13].

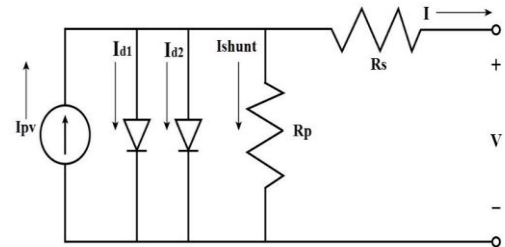


Fig. 2. Two-diode model circuit of solar cell

PV array is built up using series and parallel connections of PV panels for matching the required power so the previous equation (1) become:

$$I = N_{par} \left\{ I_{PV} - I_o \left[\exp \left(\frac{\left(\frac{V}{N_{ser}} \right) + \left(\frac{IR_s}{N_{par}} \right)}{a_1 V_{T1}} \right) + \exp \left(\frac{\left(\frac{V}{N_{ser}} \right) + \left(\frac{IR_s}{N_{par}} \right)}{a_2 V_{T2}} \right) - 2 \right] - \left(\frac{V \left(\frac{N_{par}}{N_{ser}} \right) - IR_s}{R_p} \right) \right\} \quad (4)$$

where

- V, I the output voltage and current of PV cell
- I_{pv} the photocurrent
- I_o, I_{o1}, I_{o2} the reverse saturation current of diode
- a, a_1, a_2 the diode quality factor of PV model
- $V_{T1} \& V_{T2}$ Thermal junction voltage of PV model
- k Boltzmann constant ($1.3806503e-23$ J/K)
- q The electron charge ($1.60217646e-19$ C)
- T the p-n junction operating temperature
- STC Standard Test conditions at (25°C and 1000W/m^2)
- ΔT the difference between T and T_{stc}
- V_{oc} Open circuit voltage (V)
- I_{sc} Short circuit current (A)
- K_i the temperature coefficient of short-circuit current (A/deg.C)
- K_v the temperature coefficient of open-circuit voltage (V/deg.C)
- N_s the number of cells in series
- N_{ser} the number of modules connected in series
- N_{par} the number of modules connected in parallel

parallels
Rs & Rp Series resistance and Shunt resistance

Fig. (3) and (4) depicted Simulation of The PV simulator based on two diode model large array (Nser =35, Npar =2) under variation of irradiation at STC temperature (25°C) and variation of temperature at STC irradiation (1000 W/m²) respectively.

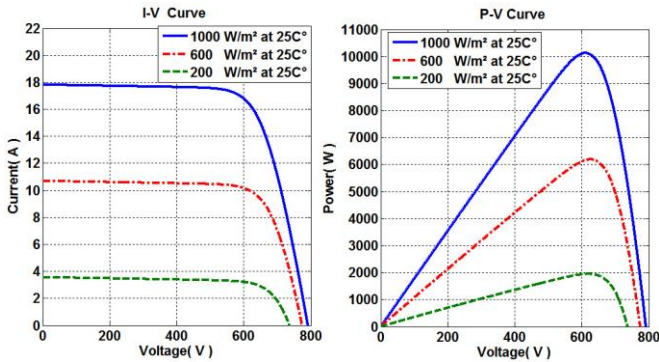


Fig. 3. I-V and P-V curves under variation of irradiation at STC temperature (25°C)

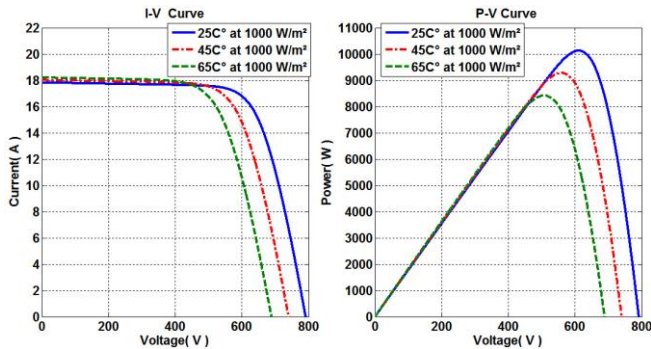


Fig. 4. I-V and P-V curves under variation of temperature at STC irradiation (1000 W/m²)

B. Estimation of DC Link Capacitor

The DC bus capacitor is estimated using the expression,

$$C_{dc} \geq \frac{P}{2\omega V_{dc} \Delta v_{dc}} \tag{5}$$

Where, V_{dc} is the reference DC voltage of VSI and P is the power injected into the motor, ω is the line angular frequency in rad/sec and Δv_{dc} is the amplitude of the DC-link voltage ripple[16, 17]. The capacitor value is selected about 3000 μF.

C. Design of the Centrifugal Pump

From the torque-speed characteristics of the three-phase IMD directly coupled with the Centrifugal Pump torque T is proportional to the square of the speed ω[18].

$$T_n = K \times \omega_n^2 \tag{6}$$

Where: T_n is the nominal torque offered by the motor and ω_n is the nominal rotational speed of the rotor in rad/sec. Therefore, the constant k should be:

$$K = T_n \times \omega_n^2 \tag{7}$$

The output power of motor is defined as:

$$P_{out} = K \times \omega^3 \tag{8}$$

The hydraulic power requirement for the pump can be calculated by equation (9)

$$P_{hyd} = g \times Q \times H \times \rho_{water} \tag{9}$$

The output power of PV array is defined as:

$$P_{PV} = V \times I \tag{10}$$

The system efficiency can be calculated in equation (11)

$$\eta_{overall} = \frac{P_{pump}}{P_{PV}} * 100\% \tag{11}$$

Where g = 9.81m/s², Q = Flow quantity (m³/s) H= Net Head (m), ρ_{water} = Density of water (kg/m³)

III. CONTROL SCHEME FOR PV PUMPING SYSTEM

Here two algorithms are implemented Adaptive Incremental Conductance (AINC) for maximum power point tracking (MPPT) and FOC for the induction machine control respectively. MPPT algorithm calculates the reference speed to be fed into FOC which used to drive motor through determines the switching strategy for the VSI.

A. MPPT CONTROL ALGORITHMS

MPPT algorithms are necessary because PV arrays have a non-linear voltage-current characteristic and the MPP of a solar panel varies with the irradiation and temperature, so the use of MPPT algorithms is required in order to obtain the maximum power from a solar array [19]. The incremental conductance algorithm is based on the fact that the slope of the curve power vs. voltage (current) of the PV module is zero at the MPP. The slope of the curve is zero, negative and positive at MPP, right side and left side of MPP respectively as shown in Fig. 5.

$$P = V \times I \tag{12}$$

$$\frac{dP}{dV} = \frac{I}{V} + \frac{dI}{dV}$$

At the maximum power point (dP/dV) should become zero and then

$$\left. \frac{dP}{dV} \right|_{MPP} = \frac{I}{V} + \frac{dI}{dV} = 0 \tag{13}$$

For any level of irradiation at the maximum power point we have:

The stator direct -axis current reference I_{ds}^* which corresponding to the stator input flux is obtained from rotor flux reference input ψ_r^* .

$$I_{ds}^* = \frac{\psi_r^*}{L_m} \quad (18)$$

At speeds higher than the rated synchronous speed of IM field weakening technique is used where I_{qs}^* increases and flux needs to be reduced in order to reduce the stator current thereby reducing the stress on the motor winding. The rotor-field angle θ_e required for coordinates transformation can be found by integrating the sum of the rotor speed ω_m and slip frequency ω_{sl}

$$\theta_e = \int (\omega_m + \omega_{sl}) dt \quad (19)$$

The slip frequency is calculated from the current command referred to the rotating q axis I_{qs} and the motor parameters.

$$\omega_{sl} = \frac{L_m \times R_r}{\psi_r \times L_r} \times I_{qs} \quad (20)$$

The I_{qs}^* and I_{ds}^* current references are converted into phase current references I_{a}^* , I_{b}^* , I_{c}^* . Where the reference currents I_{a}^* , I_{b}^* , I_{c}^* and the measured currents I_a , I_b , I_c are compared using hysteresis comparator to generate inverter gate signals[21].

IV. MATLAB MODELLING AND SIMULATION RESULTS.

Matlab/Simulink for proposed mathematical model of the PV pumping system under variable solar radiation (G) and ambient temperature (T) is presented in Fig.7 where the Photovoltaic array and other blocks have been modelled mathematically. Which beneficial to calculate the reference speed at the maximum power point as the part of MPPT technique to be fed into FOC which used to drive motor and to show the characteristics curves at different temperature and irradiance levels.

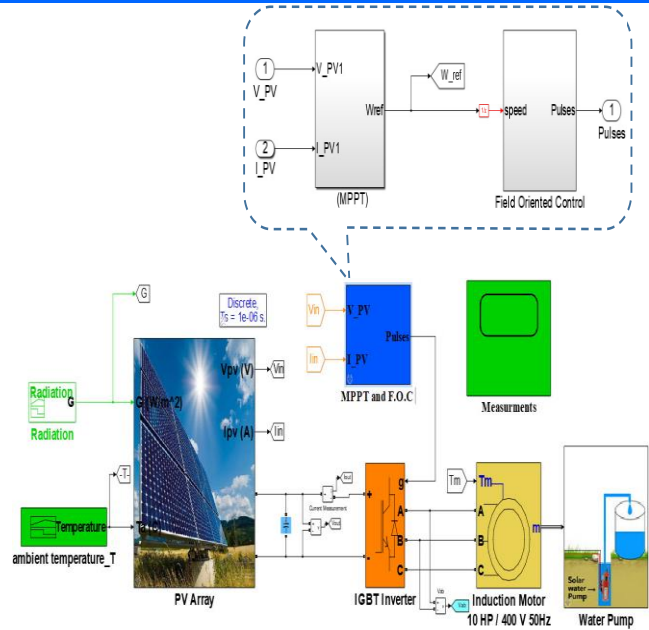


Fig.7. Matlab/Simulink of the PV pumping system under variable temperature and radiation levels.

The module data of the PV simulator based on two diode model at STC Conditions 25°C, AM1.5, and 1000 W/m² is shown in table 1.

TABLE 1. PV module Parameter.	
Parameter	Values
Ns	36
Isc (A)	8.93
Voc(V)	22.66
Current at MPP, Imp (A)	8.25
Voltage at MPP, Vmp(V)	17.54
Io1=Io2(A)	2.04667641e-10
Rp (Ω)	129.520708
Rs (Ω)	0.30

The PV array design values at STC Conditions 25°C, AM1.5, and 1000 W/m² is shown in table 2.

TABLE 2. PV array data.	
Voltage at MPP, Vmp_array(V)	614 V
Current at MPP, Imp_array (A)	16.5A
Power at MPP, Pmp_array(W)	10KW
Nser (No. of modules connected in series)	35
Npar (No.of modules connected in parallels)	2

The induction motor used in this study of the PV water pumping system coupled to a pump capable of

supplying a daily average of 47 m³/ hr at a head of 30m[22] and its parameters is shown in table 3.

Parameter	Value
Nominal power	7.5 kW
Nominal line-to-line voltage	400 V
Nominal frequency	50 Hz
Stator resistance and inductance	0.7384Ω , 0.003045H
Rotor resistance and inductance	0.7402Ω , 0.003045H
Mutual inductance	0.1241H
Number of pole pairs	2

Under different conditions of solar radiation the performance of the PV pumping system is analyzed in starting, steady state and with varying solar radiation based on the simulated results. Simulated results show that the systems performs quite satisfactorily.

A. Characteristics of the System at Starting.

The characteristics of the PV pumping system at starting period is shown in fig.8 where the radiation is increased from (0 W/m²) at t=0s to (900 W/m²) at t=0.8s. The drive system is fed power from PV array while extracting the maximum power by using Incremental conductance (MPPT) technique which calculates the reference speed to be fed into FOC which used to drive motor through determines the switching strategy for the VSI. During this period the speed will change depending on the radiation values, since the temperature is constant at 25°C. So when the radiation increased from zero to 900 W/m², the speed increased from zero to about 148 rad/s, as well as the power, voltage and current will increase.

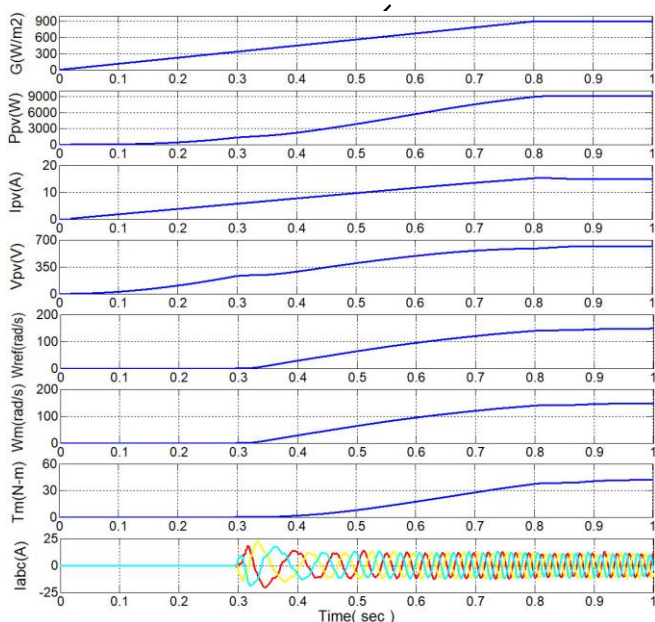


Fig.8. The characteristics of the system at starting from (0 W/m²) at t=0s to (900 W/m²) at t=0.8s.

B. Characteristics of the System at Steady State.

The characteristics of the PV pumping system at steady state period is shown in fig.9 where the radiation is fixed at 900W/m². The voltage and current of PV array are at its maximum value. The power output from the PV array determined the speed and torque of the drive.

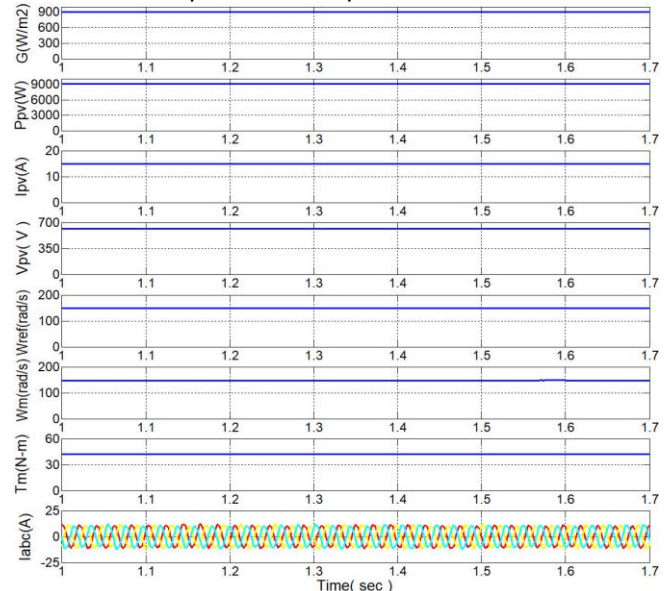


Fig.9. The steady state characteristics of the system at 900W/m².

C. Characteristics of the System at Decreasing Radiation.

The characteristics of the PV pumping system with decreasing radiation from 900W/m² to 600 W/m² at t= 1.8 s is shown in fig.10. When radiation decreases the current and the power from PV array reduces while there is not much significant drop in PV voltage. At low radiation, maximum power that can be extracted becomes less and hence there is a reduction in the reference speed of the drive. Since, torque is a function of rotor speed, there is a dip in the torque output, thereby reducing the water flow from pump.

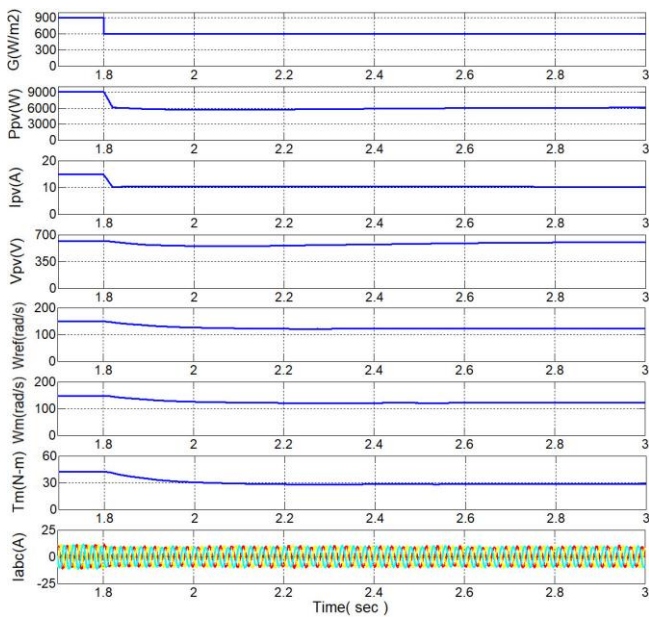


Fig.10. The characteristics of the system at radiation decrease from 900W/m^2 to 600W/m^2 at $t=1.8\text{ s}$.

The characteristics of the PV pumping system during all periods are shown in fig.11. The output power of pv array, the Motor currents, power, torque, reference speed, motor speed, pump power and quantity of output water are shown under different radiation.

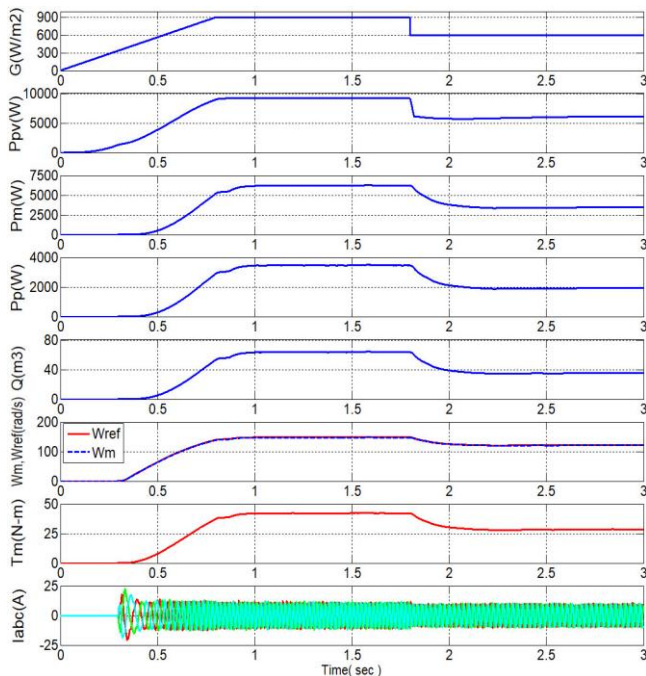


Fig.11. The characteristics of the PV pumping system during all periods

V. CONCLUSION

Modelling, simulation and analysis of PV water pumping system is presented in this paper. An

incremental conductance method is used for extraction of maximum power and the vector control is used to drive motor which provides smooth startup and reducing of starting current. The proposed system could be employed in agricultural irrigation under any operating condition of varying natures of solar irradiances and temperatures. Through this work, it can be proved that solar water pumping system is an efficient solution for helps the desert development and support of the Egyptian economy. Simulation results show the characteristics of the PV pumping system under different conditions of solar radiation, also the performance of induction motor drive satisfactorily during dynamic and steady-state conditions.

REFERENCE

- [1] M. E. Ropp and S. Gonzalez, "Development of a MATLAB/Simulink model of a single-phase grid-connected photovoltaic system," *IEEE transactions on Energy conversion*, vol. 24, pp. 195-202, 2009.
- [2] Ministry of Electricity and Renewable Energy (New & Renewable Energy Authority (NREA)), "Annual Report April 2015 of (NREA) <http://www.nrea.gov.eg/annual%20report/Annual%20Report%202015.pdf>."
- [3] H. M. Metwally and W. R. Anis, "Performance analysis of PV pumping systems using switched reluctance motor drives," *Energy conversion and management*, vol. 38, pp. 1-11, 1997.
- [4] N. Hamrouni, M. Jraidi, and A. Chérif, "Solar radiation and ambient temperature effects on the performances of a PV pumping system," *Revue des Energies Renouvelables*, vol. 11, pp. 95-106, 2008.
- [5] B. K. Bose, *Power electronics and motor drives: advances and trends*: Academic press, 2006.
- [6] D. Casadei, F. Profumo, G. Serra, and A. Tani, "FOC and DTC: two viable schemes for induction motors torque control," *IEEE transactions on Power Electronics*, vol. 17, pp. 779-787, 2002.
- [7] R. Krishnan, *Electric motor drives: modeling, analysis, and control*: Prentice Hall, 2001.
- [8] N. Mohan, *Advanced electric drives: analysis, control, and modeling using MATLAB/Simulink*: John wiley & sons, 2014.
- [9] N. Rebei, A. Hmidet, R. Gammoudi, and O. Hasnaoui, "Implementation of photovoltaic water pumping system with MPPT controls," *Frontiers in Energy*, vol. 9, pp. 187-198, 2015.
- [10] B. Subudhi and R. Pradhan, "A comparative study on maximum power point tracking techniques for photovoltaic power systems," *IEEE Transactions on Sustainable Energy*, vol. 4, pp. 89-98, 2013.
- [11] K. Ishaque, Z. Salam, and H. Taheri, "Simple, fast and accurate two-diode model for photovoltaic modules," *Solar Energy Materials and Solar Cells*, vol. 95, pp. 586-594, 2011.

- [12] C. t. Sah, R. N. Noyce, and W. Shockley, "Carrier Generation and Recombination in P-N Junctions and P-N Junction Characteristics," *Proceedings of the IRE*, vol. 45, pp. 1228-1243, 1957.
- [13] K. Ishaque, Z. Salam, and Syafaruddin, "A comprehensive MATLAB Simulink PV system simulator with partial shading capability based on two-diode model," *Solar Energy*, vol. 85, pp. 2217-2227, 9// 2011.
- [14] I. Kashif, S. Zainal, and T. Hamed, "Accurate MATLAB Simulink PV System Simulator Based on a Two-Diode Model," *JOURNAL OF POWER ELECTRONICS*, vol. 11, pp. 179-187, 2011.
- [15] K. Ishaque, Z. Salam, and H. Taheri, "Modeling and simulation of photovoltaic (PV) system during partial shading based on a two-diode model," *Simulation Modelling Practice and Theory*, vol. 19, pp. 1613-1626, 2011.
- [16] S. B. Kjaer, J. K. Pedersen, and F. Blaabjerg, "A review of single-phase grid-connected inverters for photovoltaic modules," *IEEE transactions on industry applications*, vol. 41, pp. 1292-1306, 2005.
- [17] N. Zakzouk, A. Abdelsalam, A. Helal, and B. Williams, "DC-link voltage sensorless control technique for single-phase two-stage photovoltaic grid-connected system," in *Energy Conference (ENERGYCON), 2014 IEEE International*, 2014, pp. 58-64.
- [18] J. R. Pottebaum, "Optimal characteristics of a variable-frequency centrifugal pump motor drive," *IEEE transactions on industry applications*, pp. 23-31, 1984.
- [19] T. Esum and P. L. Chapman, "Comparison of photovoltaic array maximum power point tracking techniques," *IEEE Transactions on Energy Conversion EC*, vol. 22, p. 439, 2007.
- [20] R. Thangaraj, T. R. Chelliah, M. Pant, A. Abraham, and C. Grosan, "Optimal gain tuning of PI speed controller in induction motor drives using particle swarm optimization," *Logic Journal of IGPL*, p. jzq031, 2010.
- [21] S. Goyat and R. K. Ahuja, "Speed Control of Induction Motor using Vector or Field Oriented Control," *International Journal of Advances in Engineering & Technology*, vol. 4, 2012.
- [22] Datasheet of LORENTZ PS9k2 C-SJ42-4, "http://kgelectric.co.za/assets/product_docs/lorentz/submersibles/datasheets/PSk2/LORENTZ_PS9k2_c-sj42-4_pi_en_ver301051.pdf."